Article

Cell Host & Microbe

Coagulase-Negative Staphylococcal Strain Prevents *Staphylococcus aureus* Colonization and Skin Infection by Blocking Quorum Sensing

Graphical Abstract

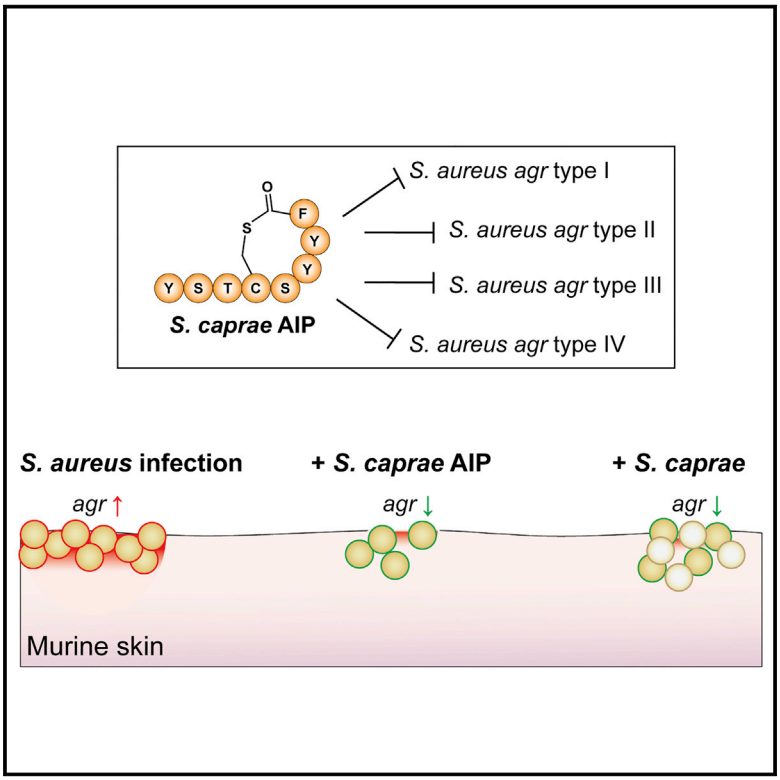

Highlights

- *Staphylococcus caprae* autoinducer (AIP) inhibits *agr* quorum sensing in *S. aureus*
- Mass spectrometry identified the *S. caprae* AIP as an eight-residue thiolactone peptide
- *S. caprae* AIP attenuates MRSA-induced necrosis and burden in a skin infection model
- *S. caprae* directly competes with MRSA during skin colonization and infection

Authors

Alexandra E. Paharik, Corey P. Parlet, Nadjali Chung, ..., Michael J. Van Dyke, Nadja B. Cech, Alexander R. Horswill

Correspondence

alexander.horswill@ucdenver.edu

In Brief

Paharik, Parlet, et al. demonstrate that the human commensal *Staphylococcus caprae* competes with *Staphylococcus aureus* by inhibiting quorum sensing. Through signal interference, *S. caprae* reduces methicillin-resistant *S. aureus* burden in both skin colonization and infection, highlighting the benefits of healthy skin flora and suggesting a new avenue for probiotic therapy.

Paharik et al., 2017, Cell Host & Microbe *22*, 746–756
December 13, 2017
https://doi.org/10.1016/j.chom.2017.11.001

CellPress

Cell Host & Microbe
Article

Coagulase-Negative Staphylococcal Strain Prevents *Staphylococcus aureus* Colonization and Skin Infection by Blocking Quorum Sensing

Alexandra E. Paharik,[1,5] Corey P. Parlet,[1,5] Nadjali Chung,[3] Daniel A. Todd,[3] Emilio I. Rodriguez,[1] Michael J. Van Dyke,[1] Nadja B. Cech,[3] and Alexander R. Horswill[2,4,6,*]
[1]Department of Microbiology, University of Iowa Carver College of Medicine, Iowa City, IA, USA
[2]Department of Veterans Affairs Denver Health Care System, Denver, CO, USA
[3]Department of Chemistry and Biochemistry, University of North Carolina at Greensboro, Greensboro, NC, USA
[4]Department of Immunology and Microbiology, University of Colorado Anschutz Medical Campus, Aurora, CO, USA
[5]These authors contributed equally
[6]Lead Contact
*Correspondence: alexander.horswill@ucdenver.edu
https://doi.org/10.1016/j.chom.2017.11.001

SUMMARY

Coagulase-negative staphylococci (CoNS) and *Staphylococcus aureus* are part of the natural flora of humans and other mammals. We found that spent media from the CoNS species *Staphylococcus caprae* can inhibit *agr*-mediated quorum sensing by all classes of *S. aureus.* A biochemical assessment of the inhibitory activity suggested that the S. *caprae* autoinducing peptide (AIP) was responsible, and mass spectrometric analysis identified the *S. caprae* AIP as an eight-residue peptide (YSTCSYYF). Using a murine model of intradermal MRSA infection, the therapeutic efficacy of synthetic *S. caprae* AIP was evident by a dramatic reduction in both dermonecrotic injury and cutaneous bacterial burden relative to controls. Competition experiments between *S. caprae* and MRSA demonstrated a significant reduction in MRSA burden using murine models of both skin colonization and intradermal infection. Our findings indicate that important interactions occur between commensals that can impact disease outcomes and potentially shape the composition of the natural flora.

INTRODUCTION

Coagulase-negative staphylococci (CoNS) are a heterogeneous group of nearly 40 species that compose the majority of the *Staphylococcus* genus (Becker et al., 2014). CoNS are generally non-pathogenic commensals of humans and other animals, and have received less attention in the literature than the more virulent *Staphylococcus aureus*. However, recent studies have described a number of interactions between CoNS and *S. aureus* that share similar host niches (Iwase et al., 2010; Janek et al., 2016; Nakatsuji et al., 2017; Sugimoto et al., 2013; Zipperer et al., 2016), demonstrating that these species can compete with *S. aureus* during colonization and potentially alter its pathogenic behavior. CoNS-*S. aureus* interactions are only beginning to be appreciated, and are important for a complete understanding of polymicrobial colonization dynamics. Investigating these interactions could shed light on the influence of the host microbiota on the ability of *S. aureus* to colonize different environments and cause disease.

S. aureus is one of the most problematic and common causes of bacterial infections (Dantes et al., 2013; Lowy, 1998; Tong et al., 2015). In particular, *S. aureus* is responsible for 76% of all skin and soft tissue infections (Moran et al., 2006), leading to 500,000 hospital visits and 10 million outpatient visits per year (Hersh et al., 2008). Infections caused by methicillin-resistant *S. aureus* (MRSA) are more difficult to treat and costly for healthcare systems (Filice et al., 2010), and the level of MRSA infections has remained high, with over 80,000 invasive infections occurring each year (Dantes et al., 2013). Community-associated MRSA (CA-MRSA) of the USA300 group have emerged as the most common isolates from skin and invasive infections (Chambers and Deleo, 2009; King et al., 2006) and are a major societal economic burden (Lee et al., 2013). In the United States alone, antimicrobial-resistant pathogens cause over two million infections per year, resulting in over 23,000 annual mortalities and leading to over $20 billion in excess medical costs (Marston et al., 2016), highlighting the need to develop innovative approaches for treatment.

Due to the major healthcare impact of *S. aureus* infections, this pathogen is the subject of ongoing discovery efforts aimed at identifying novel antimicrobial and anti-virulence treatments (Cech and Horswill, 2013; Daly et al., 2015; Munguia and Nizet, 2017; Quave and Horswill, 2014; Spellberg et al., 2013; Sully et al., 2014). *S. aureus* has several global regulators that control the production of its virulence factors, and one such regulator is the *agr* quorum-sensing system, which the staphylococci use to coordinate behavior in response to an autoinducing peptide (AIP) signal (Kavanaugh and Horswill, 2016; Thoendel et al., 2011). The *agr* system has been extensively characterized in terms of the genes regulated, functions in virulence, interactions with other global regulatory systems, and variability across the genus (Novick and Geisinger, 2008; Thoendel et al., 2011). Briefly, the

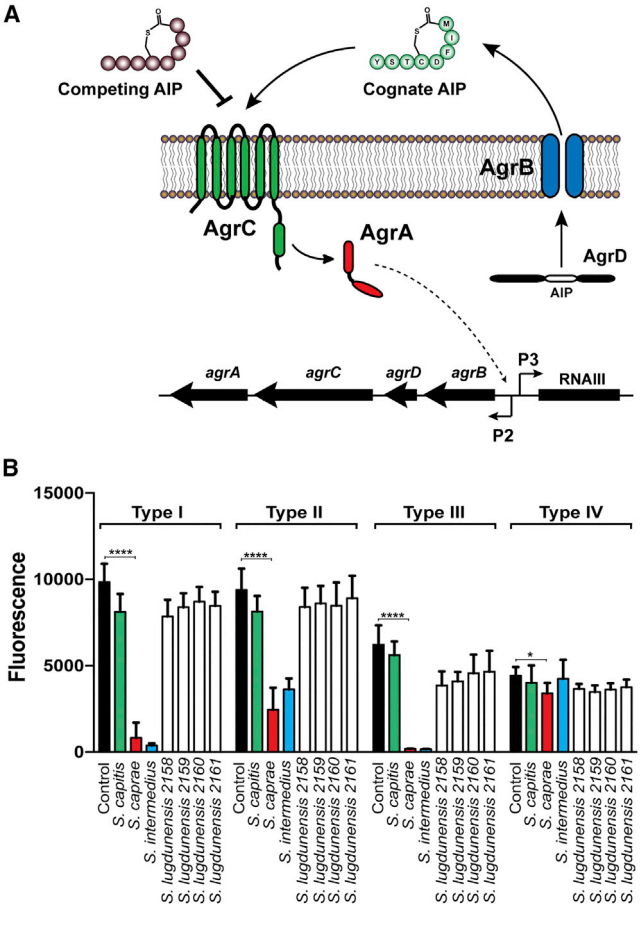

Figure 1. *S. caprae* Inhibits All Classes of *S. aureus* Quorum Sensing

(A) Schematic of *agr* system operon. Staphylococcal autoinducing peptides (AIPs) are processed and secreted in an AgrB-dependent process. Binding of the cognate AIP to AgrC results in phosphotransfer to AgrA, which induces transcription at the P2 and P3 promoters of the *agr* operon and RNAIII, respectively. Non-cognate staphylococcal AIPs can bind to AgrC and prevent signal transduction.

(B) Screen of clinical coagulase-negative staphylococcal (CoNS) isolates for inhibition of *S. aureus agr* type I–IV P3-GFP reporter. CoNS spent media were added to 10% final, and the 24 hr fluorescence time point is shown. Results are pooled from three experiments, each with n = 4 replicates per condition. Two-way ANOVA with multiple comparisons (Dunnett's correction) was performed. ****$p < 0.0001$, *$p < 0.05$.

agrBDCA operon encodes the proteins (AgrB and AgrD) needed to produce the AIP signal, as well as a two-component system (AgrC and AgrA) that senses the AIP (Figure 1A). When the AIP reaches a sufficient local concentration, it binds to the extracellular face of the AgrC histidine kinase, activating this kinase, which in turn phosphorylates the response regulator AgrA. AgrA then binds to the chromosomal P2 and P3 promoter regions to upregulate transcription of the *agrBDCA* operon and the RNAIII effector molecule, respectively, and in turn RNAIII induces global changes in gene expression (reviewed in Novick and Geisinger, 2008; Thoendel et al., 2011).

Every staphylococcal species contains an *agr* locus and produces a unique AIP molecule that varies in sequence and length. All known staphylococcal AIPs contain a five-membered thiolactone or lactone ring with an N-terminal extension, and they range in full length from 7 to 12 amino acids (Olson et al., 2014; Thoendel et al., 2011). Non-cognate AIPs have been shown to inhibit AgrC activation of AgrA, a phenomenon initially referred to as "bacterial interference" (Ji et al., 1997). Intraspecies crosstalk has been examined extensively in different *agr* types of *S. aureus* and *S. epidermidis* (Ji et al., 1997; Olson et al., 2014). However, interspecies crosstalk has received less attention, especially considering the depth and diversity of CoNS species (Becker et al., 2014). Otto and colleagues first observed that *S. epidermidis* AIP type I inhibits *S. aureus* quorum sensing, although this was only potent in *agr* type III strains (Otto et al., 2001). Since this initial observation, there have been several reports that interspecies *agr* interactions occur (Canovas et al., 2016; Geisinger et al., 2009; Ji et al., 2005; Sung et al., 2006), but in many cases, the CoNS AIP structure has not been experimentally determined, but rather predicted based on sequence.

Recently, a screen with a number of animal CoNS isolates identified several that affected *S. aureus agr* function (Canovas et al., 2016). We performed our own initial screen and identified species of CoNS whose spent media repressed *S. aureus agr*. One of the intriguing CoNS isolates that inhibited *S. aureus agr* function was *Staphylococcus caprae*, which was originally isolated from goat milk and is considered to be a commensal of goats and sheep (Devriese et al., 1983). However, recent studies have identified *S. caprae* on the skin of healthy humans (Cosseau et al., 2016; Gao et al., 2007; Kwaszewska et al., 2014), indicating that it may reside in a similar host environment as *S. aureus*. Little is known about the *S. caprae agr* system, although predictions based on AgrD gene sequence suggest that it has two *agr* types that result in different AIP structures (Thoendel et al., 2011; Zheng et al., 2015).

In this work, we characterized the *S. caprae* inhibitory activity and further investigated its impact on *S. aureus* colonization and pathogenesis. Genetic and biochemical characterization indicated that the inhibitor is the native *S. caprae* AIP, and mass spectrometry analysis of spent media revealed its structure. A synthetic version of the AIP was a potent inhibitor of *S. aureus* quorum sensing, and it prevented the progression of MRSA skin infection in a murine model. *S. caprae* successfully competed against *S. aureus* in colonization and infection models, suggesting *S. caprae* may have beneficial protective properties as a human commensal.

RESULTS

Commensal Staphylococcal Strains Secrete Inhibitors of *S. aureus* Quorum Sensing

To test for crosstalk between staphylococcal strains, we selected a small group of CoNS clinical isolates and assessed whether their spent media impacted *S. aureus* quorum-sensing function. *Staphylococcus epidermidis* has already been tested in depth (Otto et al., 1999, 2001), and thus we focused on other staphylococcal species. For reporters, we used *S. aureus* strains representing all four *agr* types containing P3 promoter YFP fusions that have been previously used to assess quorum-sensing activity (Kirchdoerfer et al., 2011; Quave et al., 2015). In our assays, *Staphylococcus capitis* and multiple clinical isolates of *Staphylococcus lugdunensis* did not affect *S. aureus*

agr activation, while *agr* P3 inhibition was observed in spent media from *Staphylococcus intermedius* and *Staphylococcus caprae* (Figure 1B). *S. intermedius* inhibited *agr* P3 activation in *S. aureus agr* types I, II, and III. The AIP from *S. intermedius* has been identified as an unusual lactone-based ring structure, and evidence that this AIP can inhibit different *S. aureus agr* types was previously noted (Ji et al., 2005). *S. caprae* spent media strongly inhibited *agr* type I, type II, and type III function in *S. aureus*. Interestingly, *S. intermedius* had no impact on *S. aureus agr* type IV (Figure 1B), while *S. caprae* was slightly inhibitory. However, type IV strains are extremely rare and often absent from culture collections (Shopsin et al., 2003). Geisinger et al. previously noted that *S. caprae* spent media had inhibitory activity against *S. aureus agr* types I and II (Geisinger et al., 2009), although the *S. caprae* AIP structure was not identified. We chose to focus our efforts on *S. caprae*, given that it is found on human skin (Cosseau et al., 2016; Gao et al., 2007; Kwaszewska et al., 2014) and may interact with colonizing *S. aureus* to provide a protective benefit to the host. Additionally, *S. caprae* has not been extensively studied, and little is known about its AIP signals or *agr* system.

S. caprae Spent Media Characterization Suggests the Inhibitory Activity Is AIP

We performed biochemical tests on the *S. caprae* spent media to gain insight into the nature of the inhibitor. The spent media did not inhibit *S. aureus* growth (Figure S1), indicating that *S. caprae* does not produce an antimicrobial agent such as those that have been recently reported in other commensal staphylococci (Janek et al., 2016; Nakatsuji et al., 2017; Zipperer et al., 2016). Next, the *S. caprae* spent media was subjected to various treatments and tested for impact on an *S. aureus agr* type I reporter. The media was exposed to heat (65°C for 1 hr), Proteinase K to degrade peptides and proteins (1 mg/mL for 1 hr), chelation with EGTA (5 mM), and NaOH (to pH 11). With the exception of NaOH-treated supernatant, all the conditions retained some inhibitory activity against *S. aureus agr* type I (Figure 2A). The thiolactone ring is critical for AIP functionality (Ji et al., 1997; Mayville et al., 1999; MDowell et al., 2001) and labile in the presence of high pH; therefore, NaOH treatment of the spent media should destroy the *S. caprae* AIP structure. Based on these preliminary observations, we hypothesized the *S. caprae* inhibitory agent might be the AIP signal.

To further characterize the *S. caprae* inhibitory properties, we used a constitutively active AgrC (R238H) mutant of *S. aureus*. AgrC (R238H) contains a point mutation in the dimerization histidine phosphotransfer subdomain of the cytoplasmic region, resulting in an "irreversibly constitutive" histidine kinase that is not inhibited by AgrC receptor antagonists (Geisinger et al., 2009). We tracked quorum-sensing induction of *S. aureus* using a quantitative assay for alpha toxin (Hla) function (Daly et al., 2015), which is induced when the *agr* system is activated. Upon treatment with *S. caprae* spent media, Hla activity decreased in *S. aureus* wild-type, but the AgrC R238H mutant retained Hla activity (Figure 2B), similar to the expected response for treatment with a competitive antagonist like AIP-II (Daly et al., 2015). Collectively, these findings indicated that the *S. caprae* inhibitory activity was likely the native AIP, and its inhibitory function was upstream of phosphorylation of AgrA.

S. caprae agrBD Are Sufficient to Inhibit Quorum Sensing in *S. aureus*

We took a genetic approach to further evaluate the hypothesis that the *S. caprae* inhibitor is an AIP. The *S. caprae* DSM 20608 type strain is not fully sequenced, but two *S. caprae agr* types have been annotated in the available sequences of *S. caprae* strains (Thoendel et al., 2011). We sequenced the *agrBD* locus of the 20608 strain and found that it encodes the sequence matching the proposed *agr* type I. To produce this peptide, we cloned *agrBD* from the *S. caprae* 20608 strain into an expression vector containing a xylose-inducible promoter (pEPSA5), resulting in the pAgrBD plasmid. Previous work has found that expression of the *agrBD* genes from a staphylococcal strain in a heterologous host is sufficient to produce an AIP (Thoendel and Horswill, 2013). We therefore expressed the pAgrBD plasmid in an *agr* deletion mutant of the strain *S. aureus* 4220, which does not make endogenous AIP. Background expression and xylose induction of this engineered strain conferred inhibitory activity against an *S. aureus agr* type I reporter strain, while induction of an empty vector control strain had no activity (Figure 2C), indicating that the *S. caprae agrBD* genes are sufficient for production of the quorum-sensing inhibitor.

Identification of the *S. caprae* AIP Structure

To identify the structure of the *S. caprae* AIP, mass spectrometry analysis of *S. caprae* spent media was performed. This experiment revealed that the native *S. caprae* type I AIP structure is 8 amino acids (YSTCSYYF, calculated *m/z* 1015.3871), with the expected C-terminal five-membered thiolactone ring characteristic of AIPs (Figure 2D). In a partially purified fraction of *S. caprae* media (eluted with 70% water/30% acetonitrile), an ion at *m/z* 1015.3836 was identified as being within 5 ppm of the calculated *m/z* of peptide YSTCSYYF (Figure 2F). Fragmentation of the 1015.3836 ion produced ions matching the mass of the predicted y_7, y_6, and y_5 fragments (Figure 2D) within 5 ppm.

Synthetic versions of the AIP and two derivative structures (+1 and −1 in N-terminal length) were obtained. Liquid chromatography-mass spectrometry (LC-MS) analysis of the synthetic eight-residue AIP matched retention time (Figure 2E), *m/z*, and fragmentation of the putative AIP from the *S. caprae* spent media (Figure 2F), confirming the assignment. Next, we tested all three of these synthetic AIPs against the *S. aureus agr* type I–IV reporters and found that each was able to inhibit *agr* function with varying efficacy (Figures 3A–3D; Table S2). The structure corresponding to the native AIP was the strongest inhibitor, with an IC_{50} of 0.6 nM against type I *S. aureus*, while the 9 and 7 aa structures inhibited with IC_{50}s of 0.83 and 3.0 nM, respectively. For all *S. aureus agr* types, the native AIP and the 9 aa structure had nearly identical activity, while the truncated 7 aa structure was significantly less inhibitory, especially against type IV (Figure 3D; Table S2).

S. caprae AIP Inhibits the Progression of a Murine MRSA Skin Infection

To investigate the potential of the *S. caprae* AIP as an anti-MRSA intervention, we evaluated its capacity to influence the infectious outcome of cutaneous challenge with the USA300 CA-MRSA strain LAC (*agr* type I, hereafter called MRSA) (Muhs et al.,

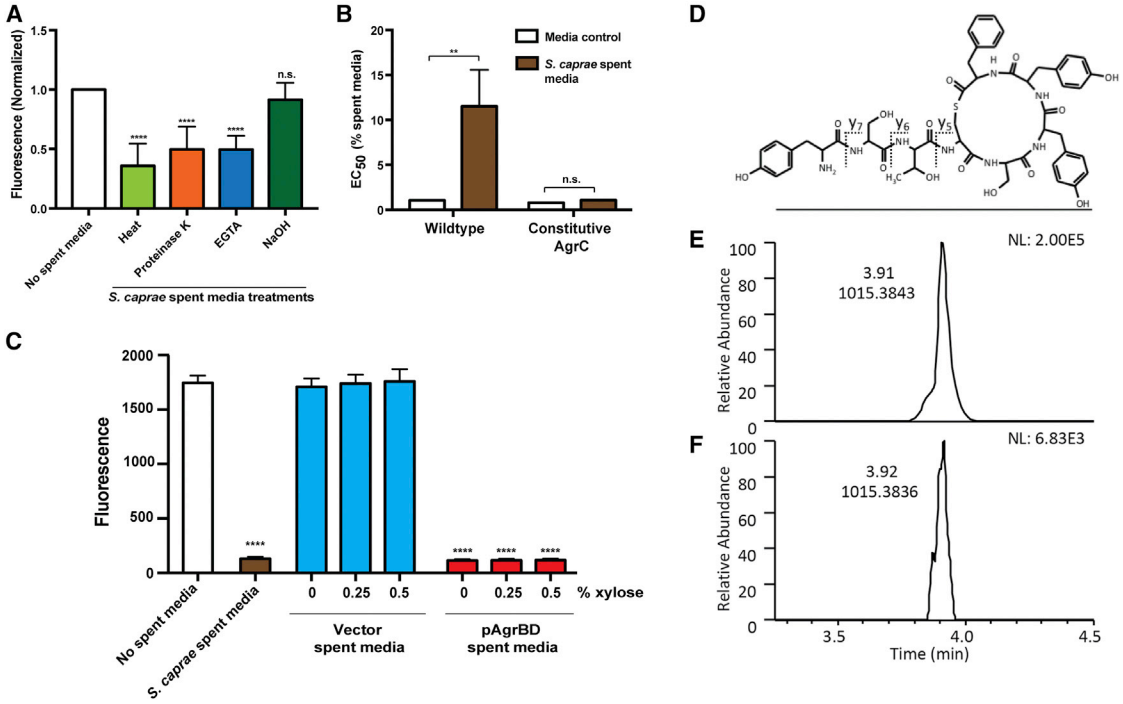

Figure 2. Initial Characterization and Identification of the *S. caprae* Quorum-Sensing Inhibitor

(A) The *S. caprae* spent media was treated with 65°C heat, Proteinase K (1 mg/mL final), EGTA (5 mM final), or NaOH (to a pH of 11, then neutralized). Each sample was added to MRSA *agr* type I reporter to 10% final and compared to no treatment control. Fluorescence was measured at 24 hr, and the results are pooled from two experiments, each with n = 3 replicates per condition, and normalized to the media control. One-way ANOVA with multiple comparisons (Dunnett's correction) was performed. ****$p < 0.0001$.

(B) Hemolysis activity assay of MRSA wild-type and constitutive AgrC (R238H) treated with *S. caprae* spent media. Activity is expressed as the percent of MRSA spent media needed to achieve 50% rabbit blood cell lysis as calculated by a four-parameter logistic curve. Results are pooled from three experiments, each with n = 3 replicates per condition. The pooled EC_{50}s were then analyzed by two-way ANOVA with each untreated versus treated pair compared (Sidak multiple comparison test). **$p < 0.01$.

(C) The *S. caprae agrBD* genes were cloned into pEPSA5 and transformed into an *S. aureus agr* deletion mutant. Spent media from this strain, and additionally an empty vector control, were tested against a MRSA *agr* type I P3-YFP reporter. The 6 hr time point is shown, and the results are pooled from two experiments, each with n = 4 replicates per condition. One-way ANOVA with multiple comparisons (Dunnett's correction) was performed. ****$p < 0.0001$.

(D) Structure of *S. caprae* AIP with predicted y_7, y_6, and y_5 fragments. The AIP is an eight-residue peptide with the last five residues constrained as a thiolactone ring.

(E) Selected ion chromatogram within ± 5 ppm of *m/z* 1015.3871 for synthetic AIP standard (retention time 3.91, measured *m/z* 1015.3843).

(F) Selected ion chromatogram within ± 5 ppm of *m/z* 1015. 3871 for 30% acetonitrile/70% water fraction of *S. caprae* spent media (retention time 3.92, measured *m/z* 1015.3836).

2017; Quave et al., 2015; Todd et al., 2017). The USA300 MRSA strains are the dominant cause of skin infection and thus serve as an appropriate output for testing (King et al., 2006; Moran et al., 2006). To this end, 5 or 10 μg of AIP was intradermally administered as part of an inoculum suspension containing MRSA. When compared to controls, AIP-treated animals exhibited significant protection from both MRSA-induced local and systemic disease as measured by dermonecrosis and weight loss, respectively (Figures 4A–4C). Highlighting the potency of AIP-mediated quorum-sensing inhibition, the cutaneous injuries sustained by AIP-treated and *agr* null challenged animals were equivalently minor in severity.

To determine if the AIP-mediated attenuation of infectious injury occurred alongside enhanced MRSA clearance, analogous challenge experiments were performed with a MRSA Lux strain for live imaging (IVIS). This approach enabled the measurement of cutaneous bacterial loads in a non-invasive and longitudinal manner. When compared to controls, AIP-treated animals exhibited a significantly lower bacterial burden throughout the course of infection (Figures 4D and 4E) and achieved levels of MRSA clearance that closely approached those observed after challenge with an *agr* null strain (Δ*agr* Lux). Representative live imaging at day 1 demonstrates the dramatic difference in MRSA burden when the *agr* communication system is intact (MRSA Lux control), completely absent (*agr* null), or profoundly disrupted (AIP-treated) (Figure 4E). Together, these data demonstrate that a single treatment of *S. caprae* AIP given at the time of infection affords significant protection against multiple disease outcomes, including tissue destruction, bacterial burden, and weight loss.

Given that direct AIP exposure does not inhibit MRSA growth *in vitro* (Figure S2), the rapid drop in MRSA burden *in vivo* suggests that within the context of infection, AIP promotes the bactericidal activity of host effector cells. Congruent with this,

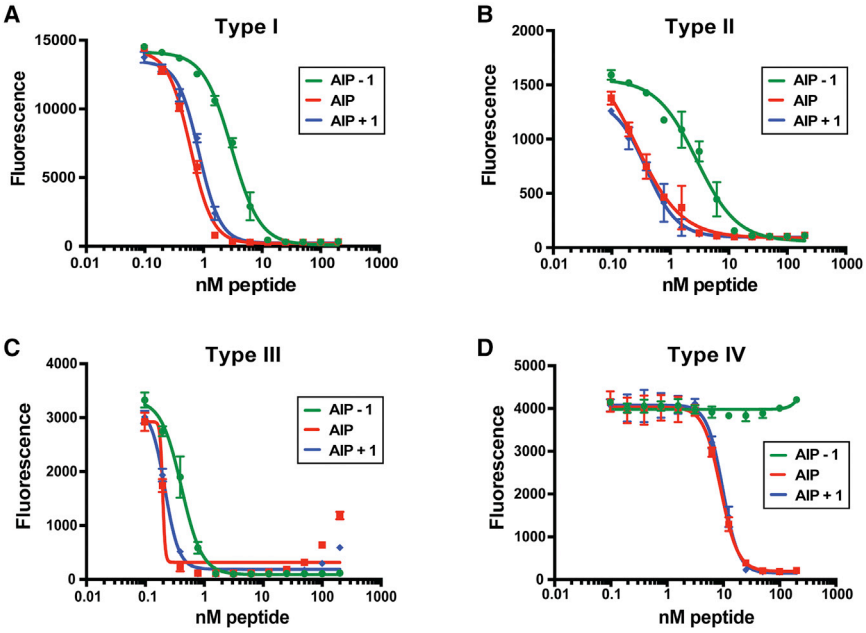

Figure 3. Inhibition of *S. aureus agr* Types I–IV with Synthetic *S. caprae* AIPs

The *agr* P3-YFP reporters of *S. aureus* types I–IV (shown in A–D, respectively) were treated with a dose response of synthetic *S. caprae* AIP, and versions with one additional residue (AIP+1) and one less residue (AIP-1) than the native structure. Fluorescence was monitored throughout growth and fitted to a four-parameter logistic curve (GraphPad PRISM 7). One representative result is shown for each reporter (n = 4 replicates per condition), and the entire experiment was repeated with similar results. Specific IC_{50} values are reported in Table S2.

we observed a profound increase in the number of neutrophils (PMNs) accumulating at the cutaneous challenge sites of AIP-treated animals relative to controls (Figure S3). Furthermore, parallel assessment of PMN phagocytosis within infected skin revealed that the AIP-induced reduction in bacterial burden corresponded with enhanced MRSA uptake by host PMNs (Figure S3). Considering that the magnitude of PMN infiltration elicited by sterile injection of AIP or vehicle was equivalent (Figure S4), it appears that the capacity of AIP to potentiate host defense is not a function of its inherent immunogenicity, but rather an indirect effect of sensitizing MRSA organisms for phagocytic clearance.

Finally, we assessed the efficacy of AIP as an intervention against established infections. To this end, at both 24 and 48 hr after MRSA Lux infection, mice were intradermally administered AIP (10 or 50 μg) at skin challenge sites. Similar to previous MRSA challenge experiments, grossly evident dermonecrosis peaked within the first 5 days following infection. Although the severity of acute injury did not differ between treatment groups, mice receiving a high dose of AIP treatment (50 μg) resolved their ulcers at an accelerated rate relative to controls. The AIP-induced promotion of cutaneous wound healing became significant late in the course of infection (>day 9 post-infection) and corresponded with reduced MRSA burden at multiple time points (Figure S5). Altogether these results show that in contrast to the overwhelming protection afforded by prophylactic AIP administration, the therapeutic effects of late-stage delivery are more subtle and manifest later during the course of infection.

S. caprae AIP Inhibits *agr* Activation during a MRSA Skin Infection

The efficacy of AIP encouraged us to better define the relationship between MRSA hypo-virulence and quorum-sensing inhibition *in vivo*. For this purpose, we carefully monitored *agr* activation kinetics within the infectious environment by intradermally challenging animals with MRSA carrying an *agr* P3-Lux reporter plasmid. Over the course of the first 5 hr of infection, exposure to *S. caprae*-derived AIP effectively blunted MRSA *agr* activation (Figures 5A and 5B). By measuring infection progression in these animals (Figure 5C), we showed that the level of AIP-mediated *agr* interference occurring during this early period after challenge corresponded with a marked attenuation of MRSA-induced dermatopathology. Histological assessment of AIP-treated and control animals (day 5 post-infection) revealed characteristic ulcerative cratering with extensive dermal necrosis and complete epidermal destruction in the latter group (Figure 5D). In contrast, the challenge sites of their AIP-treated counterparts were typified by narrow bands of necrosis that were restricted to the boundary of a highly consolidated dermal mass of inflammatory cells, all which was overlaid by an intact epidermis. Altogether, these data show that AIP-mediated quorum quenching *in vivo* profoundly attenuated the pathologic outcome of MRSA infection.

S. caprae Provides Protection during Skin Colonization and Infection Competition

When *S. caprae* and MRSA occupy the same host environment, signaling crosstalk and competition for resources could potentially influence colonization and infection progression. To address this possibility, we performed a series of co-inoculation experiments, mixing *S. caprae* and MRSA Lux in a 1:1 ratio, within settings of cutaneous carriage or invasive infection. Following epicutaneous application of both strains, a significant enhancement of early MRSA clearance (day 1) was noted using live imaging (Figures 6A and 6C), without marked injury (Figure 6B). Consistent with the known transient nature of *S. aureus* colonization in immune competent mice (Hashimoto et al., 2004), we observed that by day 4 the bioluminescence signals were quite low (Figure 6C), and by day 5 had reached baseline, indicating that bacterial clearance had occurred.

To assess the capacity of *S. caprae* to impact the outcome of an outright MRSA infection, equal colony-forming units (CFUs) of both strains (*S. caprae* and MRSA *agr* P3-Lux) were administered as part of the same inoculum suspension. Despite effectively doubling the incoming bacterial load, when compared to single-culture infections, the presence of *S. caprae* afforded

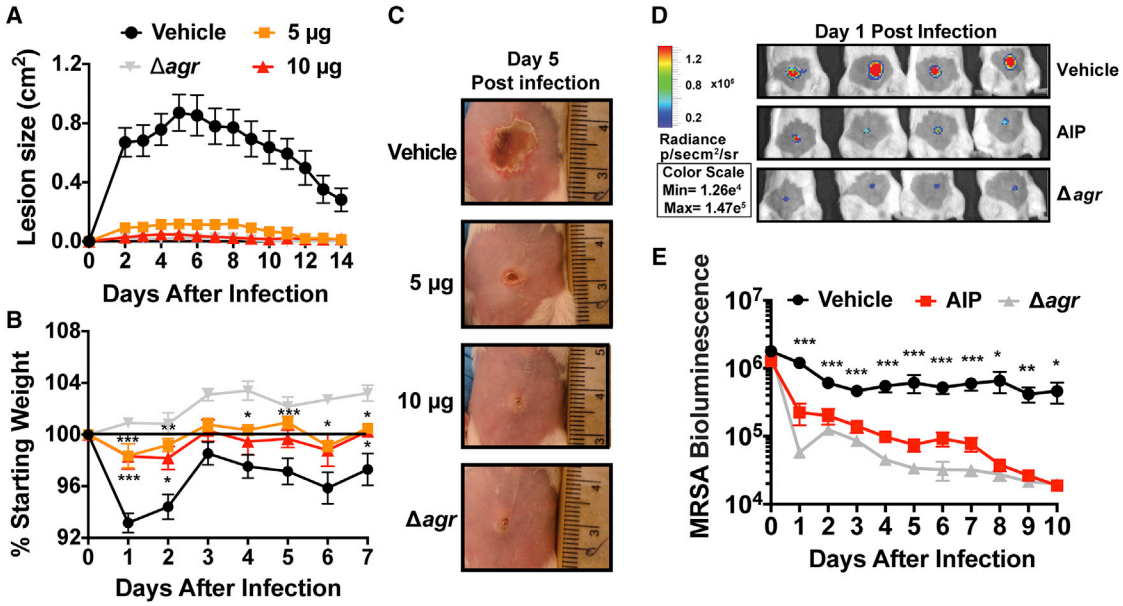

Figure 4. *S. caprae* AIP Attenuates MRSA Pathogenesis

(A) Dermonecrotic lesion size following infection with MRSA wild-type ± *S. caprae* AIP (n = 4–8). Error bars represent SEM. For every indicated time point, post-test $p < 0.0005$ for comparisons of lesion size reduction resulting from both 5 and 10 μg AIP treatments.

(B) Weight loss measurements following infection for the indicated groups (n = 4–8). Error bars represent SEM. Post-test *$p < 0.05$, **$p < 0.01$, **$p < 0.005$, ***$p < 0.001$.

(C) Representative images of tissue injury following infection with MRSA wild-type ± the indicated amounts of *S. caprae* AIP or *agr* null strain 5 days after infection.

(D) Representative images of *in vivo* bioluminescence induction 1 day after challenge with MRSA constitutive Lux ± 10 μg *S. caprae*-AIP or a Δ*agr* MRSA Lux.

(E) Time course comparison of *in vivo* bioluminescence after intradermal challenge with MRSA Lux ± 10 μg *S. caprae*-AIP or a Δ*agr* MRSA Lux (n = 8–12). Error bars represent SEM. Post-test *$p < 0.05$, **$p < 0.01$, ***$p < 0.001$.

striking protection against MRSA pathogenesis (Figures 7A and 7B). By using the MRSA *agr* P3-Lux reporter for these challenges, we were able to show the equivalent efficacy of both the synthetic AIP and *S. caprae* bacteria during the first 5 hr of infection (Figure 7C). Monitoring of the infection for 12 days showed the continued effectiveness of synthetic AIP and *S. caprae* bacteria (Figure 7D).

As a control, analogous challenge experiments were performed with a closely related CoNS species, *Staphylococcus capitis*, which did not inhibit *S. aureus agr* function during *in vitro* testing (Figure 1B). Compared to *S. caprae*, the attenuation of MRSA virulence and *agr* activity with *S. capitis* organisms was minimal compared to vehicle control (Figures 7A–7D), indicating these properties are specific to *S. caprae* and cannot be broadly generalized throughout the genus. Taken together, these data demonstrate the ability of the *S. caprae* to employ *agr* antagonism as means to oppose both the commensal carriage and pathogenic invasion of MRSA in a cutaneous environment.

DISCUSSION

Infections from the bacterial pathogen *S. aureus* place a tremendous burden on our healthcare system (Dantes et al., 2013; Lowy, 1998; Tong et al., 2015). Often termed a pathobiont, *S. aureus* is both a potent bacterial pathogen and a common constituent of human cutaneous and mucosal flora that persistently colonizes 20% of the healthy adult population (Kluytmans et al., 1997). Given that colonization is a known risk factor for invasive autoinfection (Dantes et al., 2013; Lowy, 1998; Tong et al., 2015), there is great interest in elucidating the ecological factors that prevent carriage of *S. aureus*, result in benign carriage, or induce a transition to invasive infection. There is growing appreciation that the quality and composition of the resident microbiota impact these different states, and that the skin microbiome can function as a natural protective barrier for the host (van Rensburg et al., 2015). As commensal bacteria colonize a specific niche and compete for resources, extensive interactions occur (Ghoul and Mitri, 2016), and competing bacteria can produce factors that limit *S. aureus* growth. For commensal CoNS species, it has been observed that *S. epidermidis* secretes a protease, and *S. lugdunensis* and other species release antimicrobials, each of which restricts *S. aureus* colonization (Iwase et al., 2010; Janek et al., 2016; Nakatsuji et al., 2017; Zipperer et al., 2016). These examples illustrate how resident commensal species directly target *S. aureus* to gain a competitive advantage for resources, thereby limiting pathogenic outgrowth and invasion within shared ecological niches.

There are some reports that targeting quorum sensing could be an effective strategy enabling commensals to reduce the fitness of their competitors (Dong et al., 2002; Fleming et al., 2006; Ghoul and Mitri, 2016). In this work, we discovered that *S. caprae* secretes an AIP signal that strongly inhibits *S. aureus* quorum-sensing function. Based on sequence analysis, Geisinger et al. predicted the *S. caprae* AIP could inhibit the AgrC

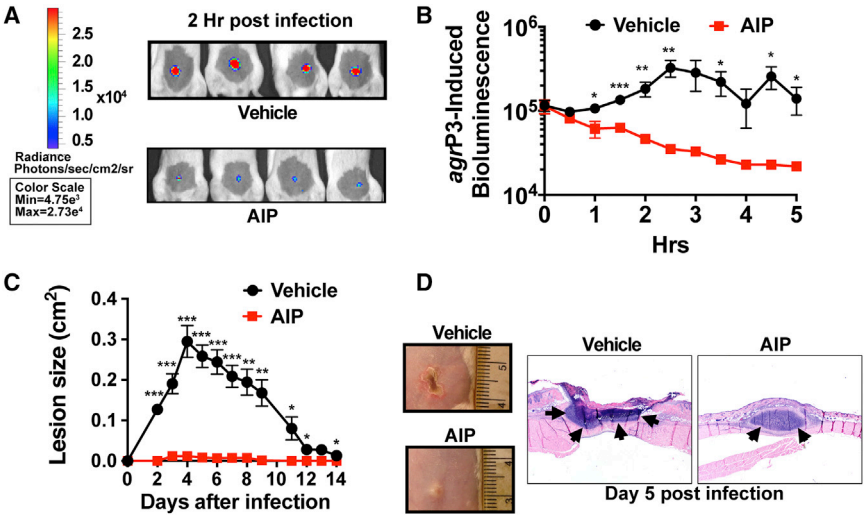

Figure 5. *S. caprae* AIP-Mediated Quorum Quenching *In Vivo* Corresponds with Protection against MRSA-Induced Dermatopathology

(A) Representative images of *in vivo* bioluminescence induction 2.5 hr after challenge with MRSA *agr* P3-Lux ± 10 μg *S. caprae* AIP.

(B) Time course comparison of *in vivo* bioluminescence after intradermal challenge with *agr* P3-Lux ± 10 μg of *S. caprae* AIP (n = 5). Error bars represent SEM. Post-test ***p < 0.005.

(C) Dermonecrotic lesion size following infection with *agr* P3-Lux ± 10 μg *S. caprae* AIP (n = 5). Error bars represent SEM. Post-test *p < 0.05, **p < 0.01, ***p < 0.001.

(D) Left: representative images showing gross appearance of gross tissue injury 5 days after infection with *agr* P3-Lux ± 10 μg *S. caprae* AIP. Right: representative hematoxylin and eosin (H&E)-stained tissue sections prepared 5 days after infection with *agr* P3-Lux ± 10 μg *S. caprae* AIP. Arrows denote distinct areas of tissue necrosis.

receptor of *S. aureus* types I and II, and demonstrated its efficacy by *in vitro* spent media testing (Geisinger et al., 2009). Our findings confirm preliminary findings by Geisinger and coworkers, and extend them to all classes of *S. aureus agr*. Using high-resolving power mass spectrometry, we directly identified the correct *S. caprae* AIP structure from the spent media, which was previously unknown. Considering that AIP tail length can be highly variable (Olson et al., 2014), and tail length strongly influences activity (Gordon et al., 2013), it is critical to directly measure the native AIP released by the bacteria to confirm its structure. Although *S. caprae* was historically regarded as a primarily animal-associates species, recent studies reveal that the presence of this microbe on human skin has been underappreciated. Knowing that *S. caprae* is present transiently on human skin (Cosseau et al., 2016; Gao et al., 2007; Kwaszewska et al., 2014), it seems likely that *S. caprae* and *S. aureus* interact within the cutaneous environment, and the production of the inhibitory AIP could give *S. caprae* a competitive advantage. In the context of these findings, our work suggests that further studies should be carried out to characterize the human skin microbiota to the species level to better appreciate the contribution of *S. caprae*. Recently, another human skin commensal, *Corynebacterium striatum*, was found to suppress *S. aureus* quorum-sensing function and showed promise in a co-infection model (Ramsey et al., 2016). These previous findings and those presented herein suggest that antagonistic crosstalk could be an effective strategy for a commensal to gain advantage in the complex skin environment.

To test the therapeutic efficacy of interspecies crosstalk, the impact of *S. caprae* AIP on MRSA skin infection progression was examined using a similar approach that was pioneered for assessment of intraspecies bacterial interference (Mayville et al., 1999). We observed profound attenuation of MRSA virulence when it was inoculated along with synthetic *S. caprae* AIP, which essentially phenocopied analogous challenges with *agr* null mutants. This success encouraged us to investigate whether the magnitude of *S. caprae* AIP production was sufficient to confer protection against MRSA within a shared host environment. The abatement of MRSA quorum sensing within the polymicrobial challenge setting suggests that *S. caprae*-derived AIP does, indeed, achieve the potency needed to blunt MRSA virulence factor induction. To explore *S. caprae*/MRSA interactions in a more natural context, we developed a model of epicutaneous administration/colonization that elicited little tissue injury and permitted longitudinal tracking of MRSA burden. Consistent with other models of colonization with immune competent mice (Hashimoto et al., 2004), we found that MRSA carriage was relatively transient. Importantly, the occupancy of MRSA upon the skin surface was substantial enough to produce a robust signal for bioluminescent imaging over a 3-day period (Figure 6). Using this approach, we observed that the presence of *S. caprae* upon the skin significantly restricted the MRSA growth and accelerated its clearance, indicating that competing commensals may serve as a means by which the microbiota restrict MRSA outgrowth and invasion.

An ongoing challenge to understanding the contribution of commensal crosstalk is that the role of *agr* during staphylococcal colonization has not received much attention. We and others have observed that the *S. aureus agr* genes are repressed during nasal colonization (Burian et al., 2010; Kiedrowski et al., 2016; Tulinski et al., 2014), but staphylococcal skin colonization has comparatively received less attention at the mechanistic level. Using a porcine skin explant model, we demonstrated that *S. epidermidis* requires quorum sensing to successfully colonize (Olson et al., 2014), suggesting the regulatory system is important for survival in this environment. Considering that every staphylococcal strain has an *agr* system (Wuster and Babu, 2008) (with varying AIP structures and receptors), it seems probable that both *S. caprae* and *S. aureus* require a functional *agr* system for skin colonization. Across all CoNS strains, the *agr* system controls production of many secreted enzymes necessary for growth on host substrates (Kolar et al., 2013; Olson et al., 2014), and controls the production of PSM peptides, which have broad-ranging properties that impact motility, host cell

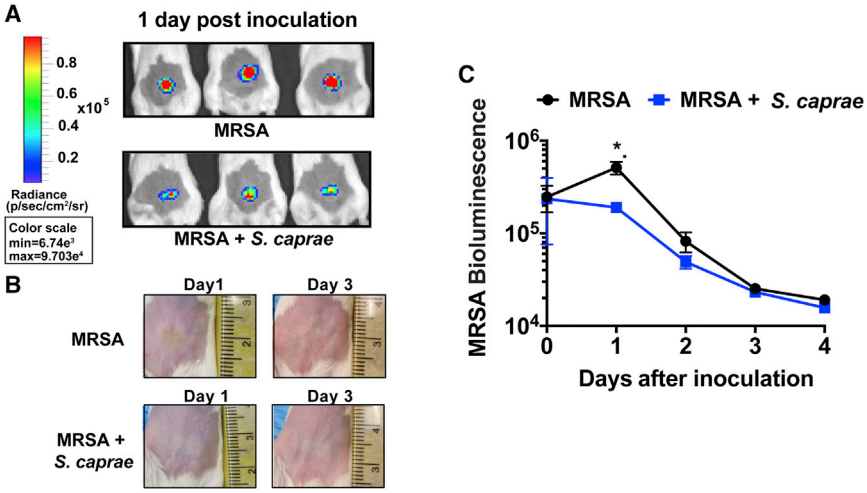

Figure 6. *S. caprae* Reduces Early MRSA Burden Following Epicutaneous Inoculation

(A) Representative images of *in vivo* bioluminescence induction 1 day after epicutaneous administration of MRSA constitutive Lux alone or together with *S. caprae*.

(B) Representative images of tissue injury following epicutaneous application of the indicated groups 1 and 3 days after challenge.

(C) Time course comparison of *in vivo* bioluminescence after MRSA mono (MRSA alone) or co (MRSA/*S. caprae*) application (n = 6). Error bars represent SEM. Post-test *p < 0.05.

lysis, and biofilm restructuring (Peschel and Otto, 2013). However, our knowledge of exo-enzyme and PSM function in most CoNS species is relatively limited. Despite these knowledge gaps, our findings with interspecies quorum-sensing antagonism suggest it could be an effective strategy for survival within a competitive host environment.

Although *S. caprae* has received little attention, its appearance in species-level analysis of skin bacterial communities suggests that its contribution as a human colonizer is underestimated (Cosseau et al., 2016; Gao et al., 2007; Kwaszewska et al., 2014). Studies to date have relied mostly on 16s rRNA sequencing, and there are inherent challenges in separating closely related species, such as each individual CoNS, and analyzing the temporal population dynamics with a single marker gene (Poretsky et al., 2014). As microbiome studies advance, our understanding of the prevalence of *S. caprae* as part of the healthy skin flora will improve, and the frequency of association or disassociation with *S. aureus* colonization will be revealed. Given that other CoNS make competing AIPs (Figure 1B; Canovas et al., 2016), and the observation that many isolates produce antimicrobials (Janek et al., 2016; Nakatsuji et al., 2017; Zipperer et al., 2016), there is clearly a network of complex, competitive interactions among commensals in the skin environment. Nakatsuji et al. recently demonstrated the importance of understanding these interactions by showing that a *Staphylococcus hominus* strain can protect atopic dermatitis patients from *S. aureus* colonization (Nakatsuji et al., 2017). This exciting advancement with *S. hominus* demonstrates the successful translation of a commensal's protective properties into an effective treatment, and it highlights the significance of investigating the contribution of normal skin flora to human health. With the post-antibiotic era looming ever closer, there is a clear need for these types of innovative scientific solutions to control antibiotic-resistant infections (Spellberg et al., 2013). It is becoming increasingly

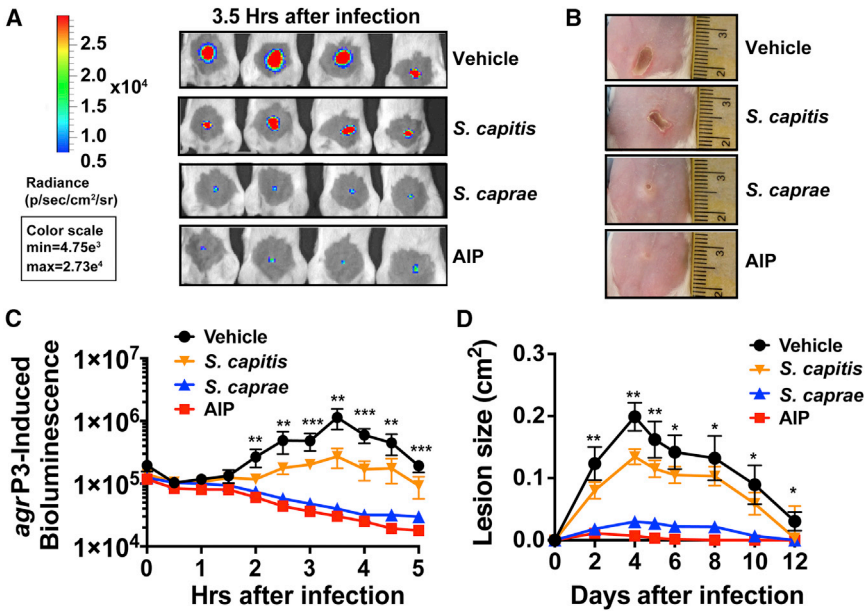

Figure 7. *S. caprae* Reduces Early MRSA Burden Following Intradermal Inoculation

(A) Representative images of *in vivo* bioluminescence induction 3.5 hr after challenge with MRSA *agr* P3-Lux ± 10 μg *S. caprae* AIP, or equal CFUs of the CoNS *S. caprae* or *S. capitis*.

(B) Representative images show dermonecrosis 5 days after the bacterial challenge.

(C) Time course comparison of *in vivo* bioluminescence after intradermal challenge within the indicated conditions (n = 5–10). Error bars represent SEM. Post-test *p < 0.05, **p < 0.01, ***p < 0.005.

(D) Time course of dermonecrotic lesion size in the indicated challenge conditions (n = 5–10). Error bars represent SEM. Post-test *p < 0.05, **p < 0.01.

clear that breakthroughs in this area may arise from the pursuit of pathogen-specific interventions that exploit specific microbial pathways, or strategies to take advantage of protective environmental conditions, such as the beneficial properties of normal flora. For *S. aureus*, a ubiquitous human pathogen with a remarkable propensity for acquiring drug resistance, there are mounting efforts to develop both of these alternative approaches into effective treatments for limiting infections.

STAR★METHODS

Detailed methods are provided in the online version of this paper and include the following:

- KEY RESOURCES TABLE
- CONTACT FOR REAGENT AND RESOURCE SHARING
- EXPERIMENTAL MODEL AND SUBJECT DETAILS
  - Bacterial Strains and Plasmids
  - Mice
- METHOD DETAILS
  - *agr* Reporter Assay
  - *S. caprae* Supernatant Treatments
  - Hemolysis Assay
  - *S. caprae* agrD Sequencing
  - pAgrBD Induction Experiment
  - Flow Cytometry
  - LC-MS Identification of *S. caprae* AIP Structure
  - Mouse Dermonecrosis Model and Colonization Models
  - Inoculum Preparation for Assessing Quorum Quenching *In Vivo*
- QUANTIFICATION AND STATISTICAL ANALYSIS
- DATA AND SOFTWARE AVAILABILITY

SUPPLEMENTAL INFORMATION

Supplemental Information includes five figures and two tables and can be found with this article online at https://doi.org/10.1016/j.chom.2017.11.001.

AUTHOR CONTRIBUTIONS

A.E.P., C.P.P., and A.R.H. designed and interpreted experiments and wrote the manuscript. A.E.P. performed the majority of the *in vitro* CoNS and AIP testing, and C.P.P. performed all of the mouse experiments. M.J.V. and E.I.R. contributed to the CoNS initial findings. D.A.T., N.C., and N.B.C. performed the mass spectrometry and contributed to editing the manuscript.

ACKNOWLEDGMENTS

We thank P. Schlievert and T. Foster for CoNS strains. We thank N. Ward for assistance with analyzing microbiome data. A.E.P. was supported by an AHA predoctoral fellowship, award number 14PRE19910005. C.P.P. was supported by NIH T32 awards AI007511 and AI007343. E.I.R. was supported by summer research NSF grant 1262222. A.R.H. is supported by a Merit Award (I01 BX002711) from the Department of Veteran Affairs and NIH public health service grant AI083211 (Project 3). The mass spectrometry analyses described herein were supported by a grant to N.C. from the University of North Carolina at Greensboro Undergraduate Research, Scholarship, and Creativity Office. The authors also thank the Comparative Pathology Laboratory at the University of Iowa for performing sectioning and staining of infected skin tissue as well as the laboratory's director, David Meyerholz, for assistance with histopathological interpretation of these preparations. The authors also thank the Central Microscopy Core and the Flow Cytometry Core facility at the University of Iowa.

Received: April 23, 2017
Revised: September 26, 2017
Accepted: October 31, 2017
Published: November 30, 2017

SUPPORTING CITATIONS

The following references appear in the Supplemental Information: Boles et al. (2010); Chiu et al. (2013); Datsenko and Wanner (2000); Figueroa et al. (2014); Forsyth et al. (2002); Heilbronner et al. (2011); Junio et al. (2013); Kreiswirth et al. (1983); Muhs et al. (2017); Pang et al. (2010); Thurlow et al. (2011).

REFERENCES

Becker, K., Heilmann, C., and Peters, G. (2014). Coagulase-negative staphylococci. Clin. Microbiol. Rev. *27*, 870–926.

Boles, B.R., Thoendel, M., Roth, A.J., and Horswill, A.R. (2010). Identification of genes involved in polysaccharide-independent *Staphylococcus aureus* biofilm formation. PLoS One *5*, e10146.

Burian, M., Rautenberg, M., Kohler, T., Fritz, M., Krismer, B., Unger, C., Hoffmann, W.H., Peschel, A., Wolz, C., and Goerke, C. (2010). Temporal expression of adhesion factors and activity of global regulators during establishment of *Staphylococcus aureus* nasal colonization. J. Infect. Dis. *201*, 1414–1421.

Canovas, J., Baldry, M., Bojer, M.S., Andersen, P.S., Grzeskowiak, P.K., Stegger, M., Damborg, P., Olsen, C.A., and Ingmer, H. (2016). Cross-talk between *Staphylococcus aureus* and other Staphylococcal species via the *agr* quorum sensing system. Front. Microbiol. *7*, 1733.

Cech, N.B., and Horswill, A.R. (2013). Small-molecule quorum quenchers to prevent *Staphylococcus aureus* infection. Future Microbiol. *8*, 1511–1514.

Chambers, H.F., and Deleo, F.R. (2009). Waves of resistance: *Staphylococcus aureus* in the antibiotic era. Nat. Rev. Microbiol. *7*, 629–641.

Chiu, I.M., Heesters, B.A., Ghasemlou, N., Von Hehn, C.A., Zhao, F., Tran, J., Wainger, B., Strominger, A., Muralidharan, S., Horswill, A.R., et al. (2013). Bacteria activate sensory neurons that modulate pain and inflammation. Nature *501*, 52–57.

Cosseau, C., Romano-Bertrand, S., Duplan, H., Lucas, O., Ingrassia, I., Pigasse, C., Roques, C., and Jumas-Bilak, E. (2016). *Proteobacteria* from the human skin microbiota: species-level diversity and hypotheses. One Health *2*, 33–41.

Daly, S.M., Elmore, B.O., Kavanaugh, J.S., Triplett, K.D., Figueroa, M., Raja, H.A., El-Elimat, T., Crosby, H.A., Femling, J.K., Cech, N.B., et al. (2015). ω-Hydroxyemodin limits staphylococcus aureus quorum sensing-mediated pathogenesis and inflammation. Antimicrob. Agents Chemother. *59*, 2223–2235.

Dantes, R., Mu, Y., Belflower, R., Aragon, D., Dumyati, G., Harrison, L.H., Lessa, F.C., Lynfield, R., Nadle, J., Petit, S., et al.; Emerging Infections Program–Active Bacterial Core Surveillance MRSA Surveillance Investigators (2013). National burden of invasive methicillin-resistant *Staphylococcus aureus* infections, United States, 2011. JAMA Intern. Med. *173*, 1970–1978.

Datsenko, K.A., and Wanner, B.L. (2000). One-step inactivation of chromosomal genes in *Escherichia coli* K-12 using PCR products. Proc. Natl. Acad. Sci. USA *97*, 6640–6645.

Devriese, L.A., Poutrel, B., Kilpper-Balz, R., and Schleifer, K.H. (1983). *Staphylococcus gallinarum* and *Staphylococcus caprae*, two new species from animals. Int. J. Syst. Bacteriol. *33*, 480–486.

Dong, Y.H., Gusti, A.R., Zhang, Q., Xu, J.L., and Zhang, L.H. (2002). Identification of quorum-quenching N-acyl homoserine lactonases from *Bacillus* species. Appl. Environ. Microbiol. *68*, 1754–1759.

Figueroa, M., Jarmusch, A.K., Raja, H.A., El-Elimat, T., Kavanaugh, J.S., Horswill, A.R., Cooks, R.G., Cech, N.B., and Oberlies, N.H. (2014).

Polyhydroxyanthraquinones as quorum sensing inhibitors from the guttates of *Penicillium restrictum* and their analysis by desorption electrospray ionization mass spectrometry. J. Nat. Prod. *77*, 1351–1358.

Filice, G.A., Nyman, J.A., Lexau, C., Lees, C.H., Bockstedt, L.A., Como-Sabetti, K., Lesher, L.J., and Lynfield, R. (2010). Excess costs and utilization associated with methicillin resistance for patients with *Staphylococcus aureus* infection. Infect. Control Hosp. Epidemiol. *31*, 365–373.

Fleming, V., Feil, E., Sewell, A.K., Day, N., Buckling, A., and Massey, R.C. (2006). Agr interference between clinical Staphylococcus aureus strains in an insect model of virulence. J. Bacteriol. *188*, 7686–7688.

Forsyth, R.A., Haselbeck, R.J., Ohlsen, K.L., Yamamoto, R.T., Xu, H., Trawick, J.D., Wall, D., Wang, L., Brown-Driver, V., Froelich, J.M., et al. (2002). A genome-wide strategy for the identification of essential genes in *Staphylococcus aureus*. Mol. Microbiol. *43*, 1387–1400.

Gao, Z., Tseng, C.H., Pei, Z., and Blaser, M.J. (2007). Molecular analysis of human forearm superficial skin bacterial biota. Proc. Natl. Acad. Sci. USA *104*, 2927–2932.

Geisinger, E., Muir, T.W., and Novick, R.P. (2009). agr receptor mutants reveal distinct modes of inhibition by staphylococcal autoinducing peptides. Proc. Natl. Acad. Sci. USA *106*, 1216–1221.

Ghoul, M., and Mitri, S. (2016). The ecology and evolution of microbial competition. Trends Microbiol. *24*, 833–845.

Gordon, C.P., Williams, P., and Chan, W.C. (2013). Attenuating *Staphylococcus aureus* virulence gene regulation: a medicinal chemistry perspective. J. Med. Chem. *56*, 1389–1404.

Hashimoto, Y., Kaneda, Y., Akashi, T., Arai, I., and Nakaike, S. (2004). Persistence of *Staphylococcus aureus* colonization on the skin of NC/Nga mice. J. Dermatol. Sci. *35*, 143–150.

Heilbronner, S., Holden, M.T., van Tonder, A., Geoghegan, J.A., Foster, T.J., Parkhill, J., and Bentley, S.D. (2011). Genome sequence of *Staphylococcus lugdunensis* N920143 allows identification of putative colonization and virulence factors. FEMS Microbiol. Lett. *322*, 60–67.

Hersh, A.L., Chambers, H.F., Maselli, J.H., and Gonzales, R. (2008). National trends in ambulatory visits and antibiotic prescribing for skin and soft-tissue infections. Arch. Intern. Med. *168*, 1585–1591.

Iwase, T., Uehara, Y., Shinji, H., Tajima, A., Seo, H., Takada, K., Agata, T., and Mizunoe, Y. (2010). *Staphylococcus epidermidis* Esp inhibits Staphylococcus aureus biofilm formation and nasal colonization. Nature *465*, 346–349.

Janek, D., Zipperer, A., Kulik, A., Krismer, B., and Peschel, A. (2016). High frequency and diversity of antimicrobial activities produced by nasal *Staphylococcus* strains against bacterial competitors. PLoS Pathog. *12*, e1005812.

Ji, G., Beavis, R., and Novick, R.P. (1997). Bacterial interference caused by autoinducing peptide variants. Science *276*, 2027–2030.

Ji, G., Pei, W., Zhang, L., Qiu, R., Lin, J., Benito, Y., Lina, G., and Novick, R.P. (2005). *Staphylococcus intermedius* produces a functional agr autoinducing peptide containing a cyclic lactone. J. Bacteriol. *187*, 3139–3150.

Junio, H.A., Todd, D.A., Ettefagh, K.A., Ehrmann, B.M., Kavanaugh, J.S., Horswill, A.R., and Cech, N.B. (2013). Quantitative analysis of autoinducing peptide I (AIP-I) from *Staphylococcus aureus* cultures using ultrahigh performance liquid chromatography-high resolving power mass spectrometry. J. Chromatogr. B Analyt. Technol. Biomed. Life Sci. *930*, 7–12.

Kavanaugh, J.S., and Horswill, A.R. (2016). Impact of environmental cues on Staphylococcal quorum sensing and biofilm development. J. Biol. Chem. *291*, 12556–12564.

Kiedrowski, M.R., Paharik, A.E., Ackermann, L.W., Shelton, A.U., Singh, S.B., Starner, T.D., and Horswill, A.R. (2016). Development of an in vitro colonization model to investigate *Staphylococcus aureus* interactions with airway epithelia. Cell. Microbiol. *18*, 720–732.

King, M.D., Humphrey, B.J., Wang, Y.F., Kourbatova, E.V., Ray, S.M., and Blumberg, H.M. (2006). Emergence of community-acquired methicillin-resistant *Staphylococcus aureus* USA 300 clone as the predominant cause of skin and soft-tissue infections. Ann. Intern. Med. *144*, 309–317.

Kirchdoerfer, R.N., Garner, A.L., Flack, C.E., Mee, J.M., Horswill, A.R., Janda, K.D., Kaufmann, G.F., and Wilson, I.A. (2011). Structural basis for ligand recognition and discrimination of a quorum-quenching antibody. J. Biol. Chem. *286*, 17351–17358.

Kluytmans, J., van Belkum, A., and Verbrugh, H. (1997). Nasal carriage of *Staphylococcus aureus*: epidemiology, underlying mechanisms, and associated risks. Clin. Microbiol. Rev. *10*, 505–520.

Kolar, S.L., Ibarra, J.A., Rivera, F.E., Mootz, J.M., Davenport, J.E., Stevens, S.M., Horswill, A.R., and Shaw, L.N. (2013). Extracellular proteases are key mediators of *Staphylococcus aureus* virulence via the global modulation of virulence-determinant stability. Microbiologyopen *2*, 18–34.

Kreiswirth, B.N., Löfdahl, S., Betley, M.J., O'Reilly, M., Schlievert, P.M., Bergdoll, M.S., and Novick, R.P. (1983). The toxic shock syndrome exotoxin structural gene is not detectably transmitted by a prophage. Nature *305*, 709–712.

Kwaszewska, A., Sobiś-Glinkowska, M., and Szewczyk, E.M. (2014). Cohabitation—relationships of corynebacteria and staphylococci on human skin. Folia Microbiol. (Praha) *59*, 495–502.

Lee, B.Y., Singh, A., David, M.Z., Bartsch, S.M., Slayton, R.B., Huang, S.S., Zimmer, S.M., Potter, M.A., Macal, C.M., Lauderdale, D.S., et al. (2013). The economic burden of community-associated methicillin-resistant *Staphylococcus aureus* (CA-MRSA). Clin. Microbiol. Infect. *19*, 528–536.

Lowy, F.D. (1998). *Staphylococcus aureus* infections. N. Engl. J. Med. *339*, 520–532.

Marston, H.D., Dixon, D.M., Knisely, J.M., Palmore, T.N., and Fauci, A.S. (2016). Antimicrobial resistance. JAMA *316*, 1193–1204.

Mayville, P., Ji, G., Beavis, R., Yang, H., Goger, M., Novick, R.P., and Muir, T.W. (1999). Structure-activity analysis of synthetic autoinducing thiolactone peptides from *Staphylococcus aureus* responsible for virulence. Proc. Natl. Acad. Sci. USA *96*, 1218–1223.

MDowell, P., Affas, Z., Reynolds, C., Holden, M.T., Wood, S.J., Saint, S., Cockayne, A., Hill, P.J., Dodd, C.E., Bycroft, B.W., et al. (2001). Structure, activity and evolution of the group I thiolactone peptide quorum-sensing system of *Staphylococcus aureus*. Mol. Microbiol. *41*, 503–512.

Moran, G.J., Krishnadasan, A., Gorwitz, R.J., Fosheim, G.E., McDougal, L.K., Carey, R.B., and Talan, D.A.; EMERGEncy ID Net Study Group (2006). Methicillin-resistant S. aureus infections among patients in the emergency department. N. Engl. J. Med. *355*, 666–674.

Muhs, A., Lyles, J.T., Parlet, C.P., Nelson, K., Kavanaugh, J.S., Horswill, A.R., and Quave, C.L. (2017). Virulence inhibitors from Brazilian peppertree block quorum sensing and abate dermonecrosis in skin infection models. Sci. Rep. *7*, 42275.

Munguia, J., and Nizet, V. (2017). Pharmacological targeting of the host-pathogen interaction: alternatives to classical antibiotics to combat drug-resistant superbugs. Trends Pharmacol. Sci. *38*, 473–488.

Nakatsuji, T., Chen, T.H., Narala, S., Chun, K.A., Two, A.M., Yun, T., Shafiq, F., Kotol, P.F., Bouslimani, A., Melnik, A.V., et al. (2017). Antimicrobials from human skin commensal bacteria protect against *Staphylococcus aureus* and are deficient in atopic dermatitis. Sci. Transl. Med. *9*, https://doi.org/10.1126/scitranslmed.aah4680.

Novick, R.P., and Geisinger, E. (2008). Quorum sensing in staphylococci. Annu. Rev. Genet. *42*, 541–564.

Olson, M.E., Todd, D.A., Schaeffer, C.R., Paharik, A.E., Van Dyke, M.J., Büttner, H., Dunman, P.M., Rohde, H., Cech, N.B., Fey, P.D., and Horswill, A.R. (2014). *Staphylococcus epidermidis agr* quorum-sensing system: signal identification, cross talk, and importance in colonization. J. Bacteriol. *196*, 3482–3493.

Otto, M., Süssmuth, R., Vuong, C., Jung, G., and Götz, F. (1999). Inhibition of virulence factor expression in *Staphylococcus aureus* by the *Staphylococcus epidermidis agr* pheromone and derivatives. FEBS Lett. *450*, 257–262.

Otto, M., Echner, H., Voelter, W., and Götz, F. (2001). Pheromone cross-inhibition between *Staphylococcus aureus* and *Staphylococcus epidermidis*. Infect. Immun. *69*, 1957–1960.

Pang, Y.Y., Schwartz, J., Thoendel, M., Ackermann, L.W., Horswill, A.R., and Nauseef, W.M. (2010). agr-Dependent interactions of *Staphylococcus aureus* USA300 with human polymorphonuclear neutrophils. J. Innate Immun. *2*, 546–559.

Parlet, C.P., Kavanaugh, J.S., Horswill, A.R., and Schlueter, A.J. (2015). Chronic ethanol feeding increases the severity of *Staphylococcus aureus* skin infections by altering local host defenses. J. Leukoc. Biol. *97*, 769–778.

Peschel, A., and Otto, M. (2013). Phenol-soluble modulins and staphylococcal infection. Nat. Rev. Microbiol. *11*, 667–673.

Poretsky, R., Rodriguez-R, L.M., Luo, C., Tsementzi, D., and Konstantinidis, K.T. (2014). Strengths and limitations of 16S rRNA gene amplicon sequencing in revealing temporal microbial community dynamics. PLoS One *9*, e93827.

Quave, C.L., and Horswill, A.R. (2014). Flipping the switch: tools for detecting small molecule inhibitors of staphylococcal virulence. Front. Microbiol. *5*, 706.

Quave, C.L., Lyles, J.T., Kavanaugh, J.S., Nelson, K., Parlet, C.P., Crosby, H.A., Heilmann, K.P., and Horswill, A.R. (2015). Castanea sativa (European chestnut) leaf extracts rich in ursene and oleanene derivatives block Staphylococcus aureus virulence and pathogenesis without detectable resistance. PLoS One *10*, e0136486.

Ramsey, M.M., Freire, M.O., Gabrilska, R.A., Rumbaugh, K.P., and Lemon, K.P. (2016). Staphylococcus aureus shifts toward commensalism in response to *Corynebacterium* species. Front. Microbiol. *7*, 1230.

Shopsin, B., Mathema, B., Alcabes, P., Said-Salim, B., Lina, G., Matsuka, A., Martinez, J., and Kreiswirth, B.N. (2003). Prevalence of *agr* specificity groups among *Staphylococcus aureus* strains colonizing children and their guardians. J. Clin. Microbiol. *41*, 456–459.

Spellberg, B., Bartlett, J.G., and Gilbert, D.N. (2013). The future of antibiotics and resistance. N. Engl. J. Med. *368*, 299–302.

Sugimoto, S., Iwamoto, T., Takada, K., Okuda, K., Tajima, A., Iwase, T., and Mizunoe, Y. (2013). *Staphylococcus epidermidis* Esp degrades specific proteins associated with *Staphylococcus aureus* biofilm formation and host-pathogen interaction. J. Bacteriol. *195*, 1645–1655.

Sully, E.K., Malachowa, N., Elmore, B.O., Alexander, S.M., Femling, J.K., Gray, B.M., DeLeo, F.R., Otto, M., Cheung, A.L., Edwards, B.S., et al. (2014). Selective chemical inhibition of *agr* quorum sensing in *Staphylococcus aureus* promotes host defense with minimal impact on resistance. PLoS Pathog. *10*, e1004174.

Sung, J.M., Chantler, P.D., and Lloyd, D.H. (2006). Accessory gene regulator locus of *Staphylococcus intermedius*. Infect. Immun. *74*, 2947–2956.

Thoendel, M., and Horswill, A.R. (2013). Random mutagenesis and topology analysis of the autoinducing peptide biosynthesis proteins in *Staphylococcus aureus*. Mol. Microbiol. *87*, 318–337.

Thoendel, M., Kavanaugh, J.S., Flack, C.E., and Horswill, A.R. (2011). Peptide signaling in the staphylococci. Chem. Rev. *111*, 117–151.

Thurlow, L.R., Hanke, M.L., Fritz, T., Angle, A., Aldrich, A., Williams, S.H., Engebretsen, I.L., Bayles, K.W., Horswill, A.R., and Kielian, T. (2011). *Staphylococcus aureus* biofilms prevent macrophage phagocytosis and attenuate inflammation in vivo. J. Immunol. *186*, 6585–6596.

Todd, D.A., Parlet, C.P., Crosby, H.A., Malone, C.L., Heilmann, K.P., Horswill, A.R., and Cech, N.B. (2017). Signal biosynthesis inhibition with ambuic acid as a strategy to target antibiotic-resistant infections. Antimicrob. Agents Chemother. *61*, https://doi.org/10.1128/AAC.00263-17.

Tong, S.Y., Davis, J.S., Eichenberger, E., Holland, T.L., and Fowler, V.G., Jr. (2015). *Staphylococcus aureus* infections: epidemiology, pathophysiology, clinical manifestations, and management. Clin. Microbiol. Rev. *28*, 603–661.

Tulinski, P., Duim, B., Wittink, F.R., Jonker, M.J., Breit, T.M., van Putten, J.P., Wagenaar, J.A., and Fluit, A.C. (2014). *Staphylococcus aureus* ST398 gene expression profiling during ex vivo colonization of porcine nasal epithelium. BMC Genomics *15*, 915.

van Rensburg, J.J., Lin, H., Gao, X., Toh, E., Fortney, K.R., Ellinger, S., Zwickl, B., Janowicz, D.M., Katz, B.P., Nelson, D.E., et al. (2015). The human skin microbiome associates with the outcome of and is influenced by bacterial infection. MBio *6*, e01315-15.

Wuster, A., and Babu, M.M. (2008). Conservation and evolutionary dynamics of the agr cell-to-cell communication system across firmicutes. J. Bacteriol. *190*, 743–746.

Zheng, B., Jiang, X., Li, A., Yao, J., Zhang, J., Hu, X., and Li, L. (2015). Whole-genome sequence of multidrug-resistant *Staphylococcus caprae* strain 9557, isolated from cerebrospinal fluid. Genome Announc. *3*, https://doi.org/10.1128/genomeA.00718-15.

Zipperer, A., Konnerth, M.C., Laux, C., Berscheid, A., Janek, D., Weidenmaier, C., Burian, M., Schilling, N.A., Slavetinsky, C., Marschal, M., et al. (2016). Human commensals producing a novel antibiotic impair pathogen colonization. Nature *535*, 511–516.

STAR★METHODS

KEY RESOURCES TABLE

REAGENT or RESOURCE	SOURCE	IDENTIFIER
Antibodies		
anti-mouse Ly6G (1A8)	Biolegend	Cat# 127614
anti-mouse CD45 (30-F11)	Biolegend	Cat# 103134
anti-mouse/human CD11b (M1/70)	Biolegend	Cat# 101226
rat anti-mouse CD16/32 FcγRIII/II (2.4G2)	Dr. Thomas Waldschmidt, Univ. of Iowa	N/A
Bacterial and Virus Strains		
Bacterial strains and plasmids, see Table S1	N/A	N/A
Biological Samples		
Rabbit defibrinated blood 250 mL	HemoStat Laboratories	Cat# DRB250
Chemicals, Peptides, and Recombinant Proteins		
Trypsin	VWR Life Sciences	Cat# 90002-07-7
Collagenase Type II	Gibo	Cat# 9001-12-1
Proteinase K 20 mg/mL	Fermentas	Cat# AM2548
Peptide STCSYYF (AIP-1)	AnaSpec	Custom synthesis
Peptide YSTCSYYF (AIP)	AnaSpec	Custom synthesis
Peptide GYSTCSYYF (AIP + 1)	AnaSpec	Custom synthesis
Tryptic Soy Agar	Difco (BD)	Cat# 236950
Tryptic Soy Broth	Difco (BD)	Cat# 211822
LB mix	RPI	Cat# L24066
Chloramphenicol	Sigma Chemical	Cat# C0378
Ampicillin	RPI	Cat# A40040
D-xylose	Sigma Chemical	Cat# X1500
PBS 1X	GIBCO	Cat# 14190-136
RPMI 1640	GIBCO	Cat# 11835-030
Lysozyme	Sigma	Cat# L6876
RNaseA	QIAGEN	Cat# 158922
Phusion High-Fidelity DNA polymerase	NEB	Cat# M0530S
BamHI restriction enzyme	NEB	Cat# R0136S
EcoRI restriction enzyme	NEB	Cat# R0101S
T4 DNA Ligase	NEB	Cat# M0202S
EGTA	RPI	Cat# E57060
NaOH pellets	Sigma Chemical	Cat# 221465
Formic Acid (Optima Grade)	Fisher Scientific	Cat# A117-50
Acetonitrile (Optima Grade)	Fisher Scientific	Cat# A955-4
Acetonitrile (HPLC Grade)	Fisher Scientific	Cat# A998SK-4
Water (Optima Grade)	Fisher Scientific	Cat# W6-4
Critical Commercial Assays		
Gentra Puregene Yeast/Bact Kit	QIAGEN	Cat# 158567
Hi-Speed Mini Plasmid Kit	IBI	Cat# IB47101
QIAquick PCR purification kit	QIAGEN	Cat# 28104
QIAquick Gel extraction kit	QIAGEN	Cat# 28704
Deposited Data		
S. caprae DSMZ 20208 *agrBD* sequence	Genomics Division, Iowa Institute of Human Genetics	GenBank: MG159799

(*Continued on next page*)

Continued

REAGENT or RESOURCE	SOURCE	IDENTIFIER
Experimental Models: Organisms/Strains		
BALB/c mice	Charles River Laboratories	Strain code 555
Oligonucleotides		
5′ GAACGAATTCTAATGAATTATGAGGAGAGT AGTAGATAAGTG 3′	Integrated DNA Technologies (IDT)	AP52
5′ GCGTGGATCCGTTATCCAATCATTCAAGC CTTCC 3′	Integrated DNA Technologies (IDT)	AP53
5′ CGTTAATGTGTCATATTGTG 3′	Integrated DNA Technologies (IDT)	AP53A
5′ CACACTTTCTGTAAATGACT 3′	Integrated DNA Technologies (IDT)	AP54A
Recombinant DNA		
See plasmids in Table S1	N/A	N/A
Software and Algorithms		
Living Image Software	Xenogen	Version 4.4
Flow Jo	TreeStar	Version 10.4
ImageJ	NIH	N/A
GraphPad PRISM	The University of Iowa	Version 7.0a
Other		
TECAN plate reader	TECAN LifeSciences	Infinite M200
Xenogen *in vivo* imaging system (IVIS)	Caliper Life Sciences	IVIS200
Barnstead Nanopure Diamond	Barnstead International	Model No: D11931
CombiFlash RF system	Teledyne-Isco	Unit ID: 625230006
Q Exactive Plus orbitrap mass spectrometer	Thermo Fisher	N/A
Acquity UPLC	Waters	Product No: Photodiode Array eλ Detector – 186015033, Column Manager – 800000247, Sample Manager – 186015006, Binary Solvent Manager - 186015001
Acquity BEH C18 UPLC column	Waters	Product No: 186002350
130 g Redisep RF C18 column	Teledyne-Isco	Cat# 69-2203-337
0.22 μM filter	Millipore	Cat# SLGS033SS

CONTACT FOR REAGENT AND RESOURCE SHARING

Further information and requests for reagents may be directed to and will be fulfilled by the Lead Contact, Alexander R. Horswill (alexander.horswill@ucdenver.edu).

EXPERIMENTAL MODEL AND SUBJECT DETAILS

Bacterial Strains and Plasmids

Strains, plasmids, and bacteriophages used in this chapter are listed in Table S1. Unless otherwise noted, strains were cultured at 37°C with 200 RPM shaking. *E. coli* was grown in Luria broth (LB) or on LB agar plates containing 100 μg/mL ampicillin to maintain plasmids when necessary. *S. aureus* and *S. caprae* were grown in tryptic soy broth (TSB) or on TSB agar plates. Staphylococcal plasmids were maintained with growth in 10 μg/mL chloramphenicol.

Mice

Male BALB/c mice were purchased from the Charles River and housed in specific pathogen free facilities at the University of Iowa. For *in vivo* studies, 8 to 20-week old age-matched mice were randomly assigned to treatment groups and at experimental end points, mice were humanely euthanized using carbon dioxide inhalation. Prior to their inclusion in the study, mice were allowed to acclimate to the ABSL-2 animal housing facility at the University of Iowa for at least seven days. The animal studies were reviewed and protocol approved by the University of Iowa Institutional Animal Care and Use Committee. The University of Iowa is AAALAC accredited, and the centralized facilities meet and adhere to the standards in the "Guide and Care of Laboratory Animals."

METHOD DETAILS

agr Reporter Assay

Overnight cultures of *S. aureus* reporter strains were grown in TSB with 10 μg/mL chloramphenicol, then subcultured at 1:200 in fresh TSB with 10 μg/mL chloramphenicol. Overnight culture of *S. caprae* was centrifuged and the supernatant was passed through a 0.22 μM filter to generate spent media. Spent media, or fresh TSB for the negative control, were added at the indicated concentrations to the reporter cultures. The final cultures were then plated at 200 μL/well into a 96-well plate and grown in a Stuart humidified incubator at 1000 RPM and 37°C. At hourly time points, plates were measured on a TECAN plate reader to quantify OD_{600} and YFP fluorescence (Ex 480/Em 515, Gain 60). For synthetic peptide addition, peptides or DMSO control were added from stocks of 20 μM in DMSO. Data from each time point were analyzed by a four-parameter logistic curve in Graphpad PRISM, where the IC_{50} is the midpoint of the curve. The IC_{50} for the time point with maximal *agr* activation is reported in Table S2, and error is reported as standard deviation.

S. caprae Supernatant Treatments

For heat treatment, *S. caprae* spent media from an overnight culture was incubated in a 65°C heat block for one hour. For proteinase K treatment, 5 μL of a 20 mg/mL proteinase K solution (Fermentas) were added to 100 μL of spent media and incubated in a 37°C heat block for one hour. For EGTA treatment, 0.5 μL of a 1M stock were added to 100 μL of spent media and incubated at room temperature for one hour. For NaOH treatment, the initial pH of the spent media was measured using 4-7 pH strips. Then, 20 μL of 10 N NaOH were added to 3 mL of spent media, achieving a pH of 11 according to a 0-14 pH strip. This spent media incubated for one hour at room temperature, then was returned to the initial pH of approximately 6.5 by adding approximately 15 μL of 37% HCl. Untreated *S. caprae* spent media also incubated at room temperature for one hour as a control. All treated supernatants were added to *S. aureus agr* type I reporter cultures at 10% vol/vol in 96-well plates as above.

Hemolysis Assay

Hla activity assay was performed as in Daly et al. (2015). Overnight cultures of LAC and the constitutive *agrC* mutant were subcultured at 1:100 in 5 mL TSB and grown for 18 hours with 10% fresh *S. caprae* spent media. Spent media from these cultures was serally diluted 2-fold across a 96-well plate. Rabbit defibrinated blood (HemoStat Laboratories) was centrifuged for ten minutes at 500 x g, 4°C to pellet rabbit erythrocytes, which were washed three times in cold PBS and resuspended to a final concentration of 3% in PBS. 30 μL of each spent media dilution was mixed with 70 μL of the erythrocyte solution in triplicate in 96-well plates, and then incubated statically at room temperature for 1 hour, after which OD_{630} was measured using a TECAN plate reader. OD_{630} versus percent spent media was plotted on a four-parameter logistic curve using Graphpad PRISM 7 and the midpoint of the curve (EC_{50}) was used as an indicator of activity.

S. caprae agrD Sequencing

Genomic DNA was isolated from the *S. caprae* strain DSMZ 20608 using the Gentra PureGene Yeast/Bact Kit (QIAGEN) according to the following modified protocol: after cells were pelleted, they were suspended in 300 μL 50 mM Tris-HCl, pH 8.0 with 100 μg/mL RNaseA (QIAGEN), and lysozyme (Sigma-Aldrich) was added to a final concentration of 50 μg/mL (instead of the QIAGEN Lytic Enzyme solution). After one hour incubation at 37°C, the manufacturer's protocol was continued, with the omission of the RNaseA step and the addition of ten-minute incubation on ice after adding the Protein Precipitation Solution. DNA was submitted for Sanger sequencing to the Iowa Institute of Human Genetics (Univ. of Iowa) using primers AP53A, sequence 5′ CGTTAATGTGTCATATTGTG 3′ and AP54A, sequence 5′ CACACTTTCTGTAAATGACT 3′. The primers were chosen from a partial sequence of *Staphylococcus caprae* strain N900362, GenBank: AF346717.1.

pAgrBD Induction Experiment

For construction of the pAgrBD plasmid, the *agrBD* genes from the *S. caprae* strain DSMZ 20608 were amplified from genomic DNA (isolated as above) using Phusion High-Fidelity DNA Polymerase (NEB) and primers AP52, sequence 5′ GAACGAATTCTAATGAAT TATGAGGAGAGTAGTAGATAAGTG 3′ and AP53, sequence 5′ GCGTGGATCCGTTATCCAATCATTCAAGCCTTCC 3′, followed by clean-up with the QIAquick PCR purification kit (QIAGEN). The resulting product and pEPSA5 were digested with EcoRI (NEB) and BamHI (NEB), gel purified using the QIAquick gel extraction kit (QIAGEN), ligated using T4 DNA ligase (NEB), and electroporated into *E. coli* BW2151. The resulting plasmid was then isolated using the HiSpeed Mini Plasmid kit (IBI) and transformed by electroporation into the *S. aureus* 4220 *agr* mutant (AH2492). To test the plasmid, *S. aureus* AH2492 containing the empty vector pEPSA5 or pAgrBD plasmid was grown in TSB with 10 μg/mL chloramphenicol. The strains were then subcultured at 1:500 in TSB with chloramphenicol and induced with xylose (from a 20% stock) at various concentrations for 14-15 hours. Spent media was obtained from these cultures and used in the reporter assay at 10% vol/vol.

Flow Cytometry

Approximately 24 hr following intradermal challenge with $1x10^8$ MRSA-GFP (+/− 10 μg AIP), or its *agr* deficient counterpart, the affected abdominal regions were carefully excised with a surgical scissors. For sterile injections of AIP or vehicle, an 8mm biopsy punch was used to remove the tissue surrounding the challenge site. In all cases, recovered tissue was incubated in trypsin

(0.6% in PBS) for 75 min at 37°C; then cut into small pieces and incubated in Collagenase type II (1 mg/mL RPMI) for 90 min at 37°C. Cell suspensions were generated by serial passage of skin fragments through 18 and 20 gauge syringes. Single cell suspensions from skin preparations were stained with the following antibodies: Anti-Ly6G (AI8), anti-CD11b (M1/70), CD45 (30-F11), which were purchased from BioLegend. To block nonspecific binding, cells were incubated with rat anti-mouse CD16/32 FcγRIII/II (2.4G2) and vortexed prior to surface staining. In all experiments, cells were collected on a FACS LSR using Diva software, and analyzed using FlowJo software. Dead cells were excluded by low forward-scatter and side-light scatter. Spectral overlaps between fluorochrome channels were corrected by automated compensation on singly stained, positive controls for each fluorochrome. In general, 50,000 cells were collected/tube.

LC-MS Identification of *S. caprae* AIP Structure

Liquid chromatography-mass spectrometry analysis of *S. caprae* spent media was performed using a similar approach to that previously described (Olson et al., 2014). This media was fractionated using a Teledyne-Isco CombiFlash RF system. Spent media (9 mL) was combined with acetonitrile (1 mL), and injected onto a 130 g Redisep RF C18 column. Sample was eluted from column using the following binary solvent gradient consisting of acetonitrile (solvent A) and water (solvent B) at a flow rate of 80 mL/min. Gradient initiated at 10% A isocratic hold for 1 column volume, then increased to 20% A and held for 1 column volume, increased to 30% and held for 1 column volume, these steps continued until solvent composition consisted of 100% A. The final step was held for 3 column volumes. Fractions were collected in 19 mL increments, and pooled based on percent B for a total of 10 fractions. Fractions were analyzed using a Waters Acquity UPLC coupled to a Thermo Fisher Q Exactive Plus orbitrap mass spectrometer. A 7 μL injection of each fraction was eluted from an Acquity BEH C18 UPLC column with the following binary solvent system containing water with 0.1% formic acid (solvent A) and acetonitrile with 0.1% formic acid (solvent B) at a 0.3 mL/min flow rate. The gradient initiated with a 0.5 min isocratic hold at 10% B. From 0.5 to 7.0 the gradient increased linearly to 60% B, followed by an isocratic hold for 0.5 min. The column was washed with 100% B and equilibrated to starting conditions from 7.5 min to 10 min. The Q-Exactive Plus was operated in the positive ion mode using the following settings: Ion source, HESI; spray voltage set, 4.0 kV; probe heater temperature, 412°C; sheath gas flow, 50; auxiliary gas, 15; sweep gas, 2; capillary temperature, 300°C; S-lens RF level, 80. A full scan experiment, scan range 500-2000, was used to identify ions matching within 5 ppm of possible AIP *m/z* values. A targeted MS^2 experiment was performed using the detected AIP *m/z* as the precursor ion, with an isolation window of 4.0 *m/z* and a normalized collision energy of 23 (arbitrary units).

Mouse Dermonecrosis Model and Colonization Models

Mice and S. aureus *Skin Challenge Model*

For intradermal challenges: Overnight cultures (grown in TSB) of USA300 MRSA strain (AH1263) constructs derived from this parental strain (e.g., Lux+ MRSA) or *S. caprae* were subcultured (1:100) in TSB and to an OD_{600} of 0.5. Bacterial cells were then pelleted and resuspended in sterile saline. For all challenge experiments the administration of bacterial cells was preceded by shaving, ethanol cleansing and performed with isoflurane anesthesia.

For AIP Efficacy Testing

50 μL inoculum suspensions containing $1x10^8$ CFUs and either *S. caprae* AIP (5 μg or 10 μg at a concentration of 10 μg/μL in neat DMSO) or DMSO alone were injected intradermally into abdominal skin using 0.3 mL/31 gauge insulin syringe (BD, Franklin Lakes, NJ). Baseline body weights of mice were measured before infection and every day thereafter for a period of 14 days. For determination of lesion size, digital photos of skin lesions were taken daily with a Canon Rebel Powershot (ELPH 330 HS) and analyzed via ImageJ software (National Institutes of Health Research Services Branch, Bethesda, MD, USA). For AIP treatment experiments, 50 μL inoculum suspensions containing $1x10^8$ CFUs MRSA Lux were injected intradermally into abdominal skin in the same fashion. At both 24 and 48 hours following infection mice received intradermal 50 μL injections of saline containing AIP (10 or 50 μg) or neat DMSO.

Colonization Competition Experiments

An established method of epicutaneous challenge was employed with modifications (Parlet et al., 2015). Briefly, 20 μL inoculum suspensions containing $1x10^8$ CFUs of both MRSA and *S. caprae* and MRSA ($2x10^8$ total organisms) or $1x10^8$ CFUs of MRSA alone was pipetted directly onto the abdomen immediately after the skin surface received 5 gentle strokes with UV irradiated 220 grit sandpaper. A gentle stream of air was then focused over the challenge site until the skin appeared moist but absent of any standing liquid. Finally, challenge sites were covered with an adhesive bandage for ≈30 minutes. For all infections, challenge dose was confirmed by plating serial dilutions of inoculum on TSA and counting ensuing colonies after overnight culture.

Inoculum Preparation for Assessing Quorum Quenching *In Vivo*

AH2759, a USA300 MRSA (LAC) strain containing the *agr* P3::*lux* reporter plasmid was tested in a manner that was similar to previously described (Muhs et al., 2017; Quave et al., 2015). The strain was grown overnight in TSB with 10 μg/mL chloramphenicol. Overnight cultures were subcultured at 1:100 in TSB with 10 μg/mL chloramphenicol and grown to an optical density of ≈0.1 at 600nm. Bacterial cells were then pelleted and resuspended in sterile saline. Inoculum suspensions containing $1x10^7$ CFUs and either 10 μg of *S. caprae* AIP, DMSO alone or an equal number *S. caprae* or *S. capitis* organisms (prepared in the prepared in the same manner) were injected intradermally into abdominal skin using 0.3 mL/31 gauge insulin syringe. As a technical control, several mice were injected in the same manner with 50 μL of sterile saline only. Beginning immediately after infection, mice were imaged under isoflurane inhalation

anesthesia (2%). Photons emitted from luminescent bacteria were collected during a 2 min exposure using the Xenogen IVIS Imaging System and living image software (Xenogen, Alameda, CA). Bioluminescent image data are presented on a pseudocolor scale (blue representing least intense and red representing the most intense signal) overlaid onto a gray-scale photographic image. Using the image analysis tools in living image software, circular analysis windows (of uniform area) were overlaid onto abdominal regions of interest (as depicted in Figure 5A) and the corresponding bioluminescence values (total flux) were measured and plotted versus time after infection. For all infections, challenge dose was confirmed by plating serial dilutions of inoculum on TSA and counting ensuing colonies after overnight culture.

QUANTIFICATION AND STATISTICAL ANALYSIS

For each experiment, the total number of replicates (N) and the statistical tests performed can be found in the figure legends. With the exception of flow cytometry data, all analyses were performed using GraphPad PRISM software version 7 (GraphPad Software, La Jolla, CA). Where multiple comparisons were used, a correction was performed to generate the highest power statistical test, as recommended by the GraphPad PRISM software. Throughout this work, significance was defined as $p < 0.05$. To compare the quorum quenching abilities of coagulase-negative strains against the four *S. aureus agr* types (Figure 1B), a two-way ANOVA with multiple comparisons (Dunnett's correction) was performed. For multiple comparisons, within every *agr* type, each treated condition was compared to the untreated control of that *agr* type.

To compare the quorum inhibitory effects of *S. caprae* spent media treated with various disruptions (Figure 2A), data from each experiment were independently normalized to the untreated *S. caprae* supernatant control, then pooled and analyzed by a one-way ANOVA with multiple comparisons (Dunnett's correction). For multiple comparisons, each treatment was compared to the untreated *S. caprae* supernatant control. To compare each *S. caprae* spent media-treated strain (wild-type or constitutive *agrC*) with its respective untreated control (Figure 2B), EC_{50}'s of the four strain conditions were independently calculated for each experiment using a four-parameter logistic curve. The pooled EC_{50}'s were then analyzed by a two-way ANOVA with each untreated versus treated pair compared (Sidak multiple comparison test). To quantify the quorum quenching effects of engineered spent media (Figure 2C), a one-way ANOVA with multiple comparisons (Dunnett's correction) was performed on the dataset as a whole, with each value compared to the untreated control. To quantify activity of the synthetic peptides (Figures 3A–3D), a four parameter logistic curve was used in PRISM to independently calculate IC_{50} for each experiment. In figures four through seven, unless otherwise noted, statistics are reported as two-tailed, unpaired Student's t tests with each treatment compared to the vehicle control.

DATA AND SOFTWARE AVAILABILITY

The accession number for the *S. caprae* sequencing data is GenBank: MG159799.